CrystEngComm

PAPER

View Article Online
View Journal | View Issue

Cite this: *CrystEngComm*, 2018, **20**, 2169

A water stable microporous metal–organic framework based on rod SBUs: synthesis, structure and adsorption properties†

Jiaqi Yuan,[a] Li Mu,[b] Jiantang Li,[a] Lirong Zhang,[a] Guanghua Li,[a] Qisheng Huo[a] and Yunling Liu *[a]

Received 15th January 2018,
Accepted 15th March 2018

DOI: 10.1039/c8ce00064f

rsc.li/crystengcomm

A novel water stable porous metal–organic framework (MOF), $[Cu_3(OH)_2(IBA)_2(CH_3COO)_2]$·DMA (**1**) (HIBA = 4-(imidazol-1-yl)-benzoic acid, DMA = *N*,*N*-dimethylacetamide), has been solvothermally synthesized and structurally characterized. The framework of compound **1** is constructed from rod SBUs with a new (5,8)-connected topology. Compound **1** exhibits exceptional chemical stability under various conditions (organic solvents, water, boiling water or pH = 1–8 acidic and basic aqueous solutions). Meanwhile, it exhibits good selectivity for CO_2 over CH_4 (6.6 for CO_2/CH_4 = 0.5/0.5 and 5.8 for CO_2/CH_4 = 0.05/0.95 under 1 bar at 298 K). The excellent stability of compound **1** is of extreme importance for its practical industrial applications.

Introduction

In the past two decades, porous metal–organic frameworks (MOFs), as an arising class of functional materials, which are made up of inorganic metal ions or clusters connected by organic linkers through coordination bonds, have gained considerable attention from both academia and industry.[1] Owing to their tunable pore size, modifiable pore surface and milder synthesis conditions, they have exhibited a wide range of potential applications (gas adsorption and separation,[2] catalysis,[3] drug delivery,[4] luminescence sensing,[5] magnetism,[6] *etc.*).

As one of the primary greenhouse gases, carbon dioxide has attracted the attention of scientists all over the world not only for its possibility to cause global warming, but also because of the troubles it can cause when using natural gas since it can lower the energy conversion rate.[7] Therefore, effective and selective adsorption of CO_2 is significant for natural gas purification.[8] MOFs, as a new class of sorbent materials, are quite qualified for such an application demand.

However, most of the earlier reported MOFs, and even some of the milestone MOFs, such as MOF-5,[9] are sensitive to water conditions due to the instability of ligand–metal bonds.[10] The structures of MOFs are vulnerable to the attack of water molecules, which might lead to phase changes, ligand displacement and structure decomposition.[11] Compared with porous carbon materials, zeolites and metal oxides, the limited thermal and chemical stability (especially water stability) of MOFs hampers their popularity in industrial applications, as water or moisture commonly exists in most industrial processes.[12] Consequently, water stable MOFs, such as UiO-66,[13] NU-1000,[14] DUT-51,[15] and MIL-127,[16] have been in great demand when considering these materials for adsorption applications. Although thousands of different MOFs have been reported in the literature, only a few of them have high chemical stability, especially water stability.

Generally, water stable MOFs can be classified into three categories: (1) metal azolate frameworks with N-donor ligands, such as zeolite-like imidazole frameworks (ZIFs);[17] (2) metal carboxylate frameworks consisting of multivalent metal ions, such as MIL-101 and UiO-66;[13,18] and (3) MOFs without open metal sites or decorated by a hydrophobic pore surface.[11a] However, only N-donor ligands, such as imidazole, can easily form mononuclear metal nodes, just like ZIFs which are normally constructed from mononuclear Zn(II), Co(II) and Cd(II). In addition, multivalent metal ions, such as Cr^{3+} and Zr^{4+}, are usually costly and need complex synthesis. Thus, in order to obtain highly stable and at the same time structurally diverse MOFs, we choose a linear ligand: HIBA (HIBA = 4-(imidazol-1-yl)-benzoic acid), which contains both carboxylate and imidazole groups in consideration of the following points: (1) the multiple coordination mode of the carboxylate groups is able to form a variety of multinuclear

[a] *State Key Laboratory of Inorganic Synthesis and Preparative Chemistry, College of Chemistry, Jilin University, Changchun 130012, P. R. China.*
E-mail: yunling@jlu.edu.cn; Fax: +86 431 85168624; Tel: +86 431 85168614
[b] *School of Bioscience and Technology, Changchun University, Changchun 130023, P. R. China*

† Electronic supplementary information (ESI) available: Materials and methods, crystal data and structure refinement, structure information, XRD, TGA, gas adsorption and adsorption selectivity. CCDC 1517751. For ESI and crystallographic data in CIF or other electronic format see DOI: 10.1039/c8ce00064f

metal nodes; (2) the N-coordination point from the imidazole group can effectively prevent the formation of open metal sites and commendably enhance the chemical and thermal stability of the framework. As a consequence, a novel water stable porous rod SBU-based metal–organic framework: $[Cu_3(OH)_2(IBA)_2(CH_3COO)_2]\cdot DMA$ (**1**), has been successfully synthesized.[19] Adjacent rod SBUs are connected with each other *via* the ligand to form a three-dimensional framework. Because of the introduction of the imidazole group and the stable rod SBUs, compound **1** has an exceptional chemical stability, especially water stability. The outstanding stability of compound **1** is necessary when considering it for practical adsorption applications.[12] In addition, the adsorption behaviour of activated compound **1** for some small gases (CO_2, CH_4 and C_2H_6) has been analysed. Ideal adsorbed solution theory (IAST) calculations have also been performed to investigate the gas selectivity.

Experimental

Materials and methods

All chemicals were obtained from commercial sources and used without further purification. Powder X-ray diffraction (PXRD) data were collected using a Rigaku D/max-2550 diffractometer with Cu-K_α radiation (λ = 1.5418 Å). Elemental analyses (C, H, and N) were performed by using a vario MICRO (Elementar, Germany). Thermal gravimetric analyses (TGA) were performed on a TGA Q500 thermogravimetric analyzer used in air with a heating rate of 10 °C min^{-1}.

Synthesis of compound 1

A mixture of $Cu(NO_3)_2\cdot 3H_2O$ (0.010 g, 0.041 mmol), HIBA (0.004 g, 0.021 mmol), DMA (1.5 mL), H_2O (0.5 mL), and HNO_3 (300 μL, 2.2 mL HNO_3 in 10 mL DMF) was added into a 20 mL glass vial. The glass vial was sonicated for 10 minutes until a clear and transparent solution was obtained. The sealed vial was heated at 105 °C for 36 hours. Green stick crystals were obtained, and then collected, washed with DMA, and dried in air. Elemental analysis (%) calc. for $C_{28}H_{34}Cu_3N_6O_{10}$: C 40.98; H 3.86; N 8.92, found: C 41.73; H 4.22; N 10.43. The experimental powder X-ray diffraction (XRD) pattern of compound **1** agrees well with the simulated one based on the single-crystal X-ray data, indicating that compound **1** is a pure phase (Fig. S1†).

X-ray crystallography

Crystallographic data for compound **1** was collected using a Bruker Apex II CCD diffractometer with graphite-monochromated Mo-K_α (λ = 0.71073 Å) radiation at room temperature. The structure was solved by direct methods and refined by full-matrix least-squares on F^2 using SHELXTL-NT version 5.1.[20] All metal atoms were located first, and then the oxygen and carbon atoms of the compound were subsequently found in difference Fourier maps. The hydrogen atoms of the ligand were placed geometrically. All non-hydrogen atoms were refined anisotropically. The final formula was derived from the crystallographic data combined with the elemental and thermogravimetric analysis data. The detailed crystallographic data and selected bond lengths and angles for compound **1** are listed in Tables S1 and S2,† respectively. Topology information for compound **1** was calculated using TOPOS 4.0.[21]

Gas adsorption measurements

N_2, CO_2, CH_4 and C_2H_6 gas adsorption measurements were performed on Micromeritics ASAP 2420, Micromeritics ASAP 2010 and Micromeritics 3-Flex instruments. Before gas adsorption measurements, the microcrystalline samples of compound **1** were exchanged with fresh ethanol 8 times for 3 days to completely remove the nonvolatile solvent molecules, which can be proved by TGA (Fig. S5†). The samples were activated by drying under dynamic vacuum at 80 °C for 30 minutes. Before gas adsorption measurements, the samples were dried again by using the 'outgas' function of the surface area analyzer for 10 hours at 120 °C.

Results and discussion

Crystal structure descriptions

Single-crystal X-ray diffraction analysis shows that compound **1** crystallizes in the monoclinic crystal system with the space group *C*2/*c*. Structural analysis reveals that there exist novel 1D infinite rod-shaped metal chain SBUs in the crystal structure. As shown in Fig. 1a, there are two types of Cu(II) atoms in the rod SBU. One is five-coordinated by two μ_3-OH, two carboxylate groups and one nitrogen atom. The other is six-coordinated by two μ_3-OH and four carboxylate groups. Saturated coordinated Cu(II) atoms are combined to form a rod-shaped metal chain, which can be simplified as a series of edge-sharing octahedra.[19a] It is worth noting that the saturated metal ions can effectively improve the stability of the structure. The angular ligand HIBA links the metal chains together to form a 3D framework. As shown in Fig. 1b and c, along the [001] direction, there exists a one-dimensional channel with a diameter of 6.2 Å × 5.3 Å considering the van der Waals radius. The position of four carboxylate carbon atoms and two nitrogen atoms can be considered to be located at the vertices of a distorted octahedron as shown in Fig. S10.† These edge-sharing octahedra consist of infinite rod SBUs, which are connected with each other through the linear ligand HIBA to form a 3D framework. The position of the N atom can be treated as a 5-c node and the C atom as an 8-c node. Thus, the whole structure can be described as a (5,8)-connected binodal network, which belongs to a new topology with a Schläfli symbol of $(3^4\cdot4^3\cdot5^2\cdot6)$ $(3^8\cdot4^9\cdot5^6\cdot6^5)$. The topological characteristics exhibited by the tiles are illustrated in Fig. 1d. The total solvent-accessible volume has been calculated using PLATON. The volume is equal to 3241.3 $Å^3$ per unit cell, which takes up approximately 24.7% of the cell volume, exhibiting porosity and offering possibilities for gas adsorption.

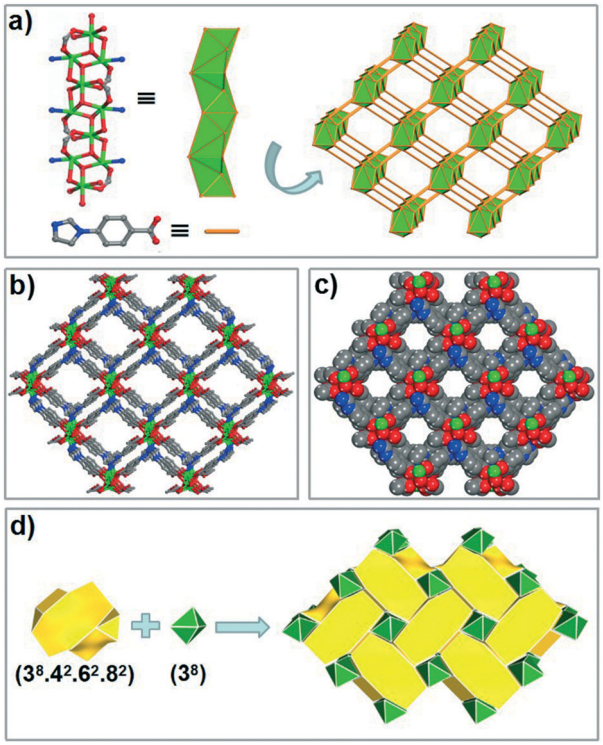

Fig. 1 Single-crystal structure of compound **1**: (a) topology simplification of the metal chain and the ligand; (b) ball and stick model of the 3D framework of compound **1** viewed along the [001] direction; (c) space-filling view of the structure of compound **1** along the [001] direction; (d) topological features of compound **1** displayed by tiles and face symbols for yellow and green are $(3^8.4^2.6^2.8^2)$ and (3^8).

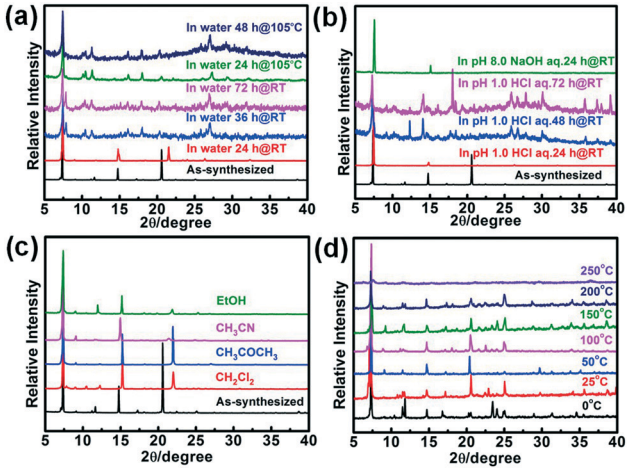

Fig. 2 PXRD patterns of compound **1**: after treatment in water at room temperature and 105 °C (a); after treatment under acidic and basic conditions (b); after being soaked in different organic solvents for one week (c); the temperature-dependent PXRD pattern (d).

Thermogravimetric and stability analysis

Thermogravimetric analysis (TGA) measurement indicated that compound **1** exhibits a three-step weight loss (Fig. S5†). The first slight weight loss of 6.8% was observed prior to 200 °C, which can be attributed to the removal of guest molecules (DMA) (calcd 6.2%).[22] The weight loss of 58.7% between 250 and 400 °C can be associated with the removal of organic ligands and structure collapse (calcd 59.2%). The last remaining weight loss at 500 °C of 29.7% is attributed to the formation of CuO (calcd 29.8%).

In order to explore the chemical stability of compound **1**, first, the as-synthesized samples of compound **1** were soaked in water at room temperature and 105 °C for 3 days, respectively. The corresponding experimental PXRD patterns indicate that the samples still retain their high crystallinity and agree well with those simulated from the single-crystal structure data (Fig. 2a), demonstrating the extraordinary water stability of compound **1**. Furthermore, the stability of compound **1** in acidic and basic aqueous solutions was investigated. As shown in Fig. 2b, the framework of compound **1** can be retained for at least 24 hours in pH 1.0 HCl and pH 8.0 NaOH solutions, and only a part collapsed after being soaked for over 48 hours. Also, compound **1** shows high stability in common organic solvents, including EtOH, CH_3CN, CH_3COCH_3 and CH_2Cl_2 (Fig. 2c). Finally, in order to confirm the thermal stability of compound **1**, temperature-dependent PXRD was conducted. As Fig. 2d shows, the samples of compound **1** can remain crystalline up to 200 °C. When it was heated to 250 °C, the framework of compound **1** partly collapsed. Combined with the above research, compound **1** has an excellent chemical and thermal stability. Compared with many well-known Cu-based MOFs, such as HKUST-1,[23] MOF-14,[24] *etc.*, compound **1** performs better in terms of chemical (especially water) stability. The notable chemical stability of compound **1** towards water, acidic and basic conditions indicates that it is a promising material for practical industrial applications.[25]

Gas adsorption and separation behaviors

To verify the porosity of compound **1**, N_2 adsorption measurement was carried out at 77 K. Fig. S2† shows a near type-I sorption isotherm for N_2 at 77 K, with an adsorption amount of 70 $cm^3\ g^{-1}$ at 1 bar. The Brunauer–Emmett–Teller (BET) surface area was calculated to be 197 $m^2\ g^{-1}$, while the Langmuir surface area was 274 $m^2\ g^{-1}$. The micropore volume is 0.11 $cm^3\ g^{-1}$, which is close to the theoretical value of 0.17 $cm^3\ g^{-1}$. In order to prove the stability of compound **1**, N_2 adsorption measurement of the water-treated samples was also carried out (Fig. S11†). The N_2 isotherm type is similar to the untreated one. The adsorption amount of N_2 is 45.5 $cm^3\ g^{-1}$ at 77 K under 1 bar, which is relatively less than the amount of untreated samples. As shown in Fig. 2a, there are some little differences in the PXRD patterns between compound **1** and the water-treated samples, indicating that the framework of compound **1** has been only partly collapsed.

The CO_2 adsorption performance was explored and the adsorption isotherms are shown in Fig. 3a. The amount of CO_2 uptake for compound **1** is 35 and 26 $cm^3\ g^{-1}$ at 273 and 298 K under 1 bar, respectively. To investigate the affinity of the framework of compound **1** to CO_2, the isosteric CO_2

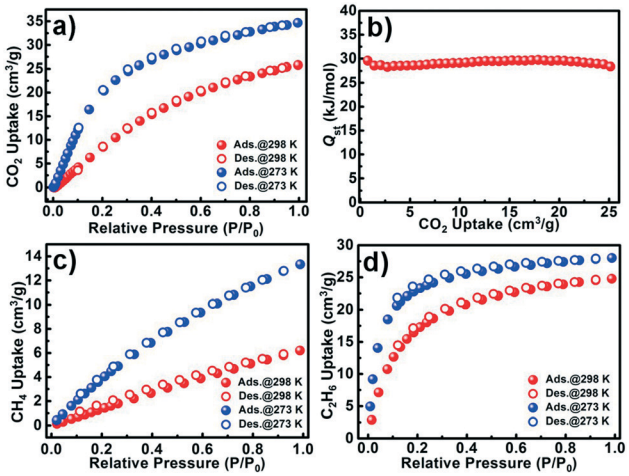

Fig. 3 CO_2 (a), CH_4 (c), and C_2H_6 (d) adsorption isotherms for compound **1** at 273 K and 298 K under 1 bar; Q_{st} of CO_2 for compound **1** (b).

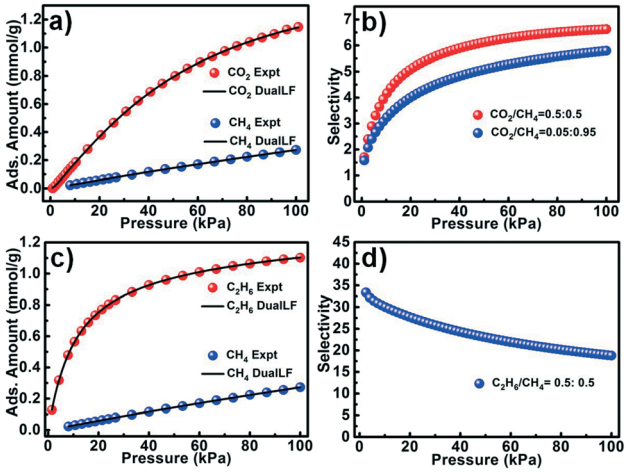

Fig. 4 CO_2, CH_4 and C_2H_6 adsorption isotherms at 298 K along with the dual-site Langmuir–Freundlich (DSLF) fits (a and c); gas mixture adsorption selectivity is predicted using IAST at 298 K and 100 kPa for compound **1** (b and d).

adsorption enthalpy (Q_{st}) on compound **1** was calculated using the virial model (Fig. 3b). Compound **1** shows a near-zero coverage with a Q_{st} value of 29.6 kJ mol^{-1}. This phenomenon indicates the strong van der Waals interactions between the framework and the gas molecules at low pressure.

Due to its good stability, compound **1** has potential storage and selective separation applications for CO_2 and small hydrocarbons (CH_4, C_2H_6, *etc.*), which are the main components of natural gas. The adsorption isotherms of CH_4 and C_2H_6 are evaluated at 273 and 298 K under 1 bar. The maximum adsorption capacities for CH_4 are 13 and 6 cm^3 g^{-1} and for C_2H_6 are 28 and 25 cm^3 g^{-1}, respectively (Fig. 3c and d). The adsorption capacity for C_2H_6 is higher than that for CH_4. This adsorption capacity trend of C_2H_6 > CH_4 is consistent with those reported in some previous studies.[26] As estimated from the sorption isotherms at 273 and 298 K, the Q_{st} values at zero coverage are 30 and 31 kJ mol^{-1} for CH_4 and C_2H_6 adsorption, respectively (Fig. S6 and S7†).

In order to evaluate the practical separation ability of compound **1** for CO_2, the gas selectivity for CO_2/CH_4 (5% and 95%, 50% and 50%) and C_2H_6/CH_4 was calculated *via* IAST, which is a common method used to calculate binary mixture gas adsorption based on experimental single-component isotherms.[27] By using the dual-site Langmuir–Freundlich equation to fit the data (Fig. 4a and c), we successfully made the models fit the isotherms at 298 K very well ($R^2 > 0.9999$).[28] Then, the fitting parameters are used to calculate the multi-component adsorption with IAST (Table S3†). As shown in Fig. 4b, the selectivity of compound **1** for CO_2 over CH_4 according to the experimental data is 6.6 and 5.8 at 298 K and 1 bar, which surpass the values for MOF-5, JLU-Liu37 (3.8),[29] ZJU-60 (5–5.5),[30] SNNU-22 (4.5) and many reported carbon materials under the same measurement conditions.[19b] Also, the potential separation application of typical small hydrocarbons is investigated for compound **1** using IAST. As shown in Fig. 4d, the selectivity for C_2H_6 over CH_4 for equimolar mixture is 19 at 298 K and 1 bar.

Conclusions

In summary, we have successfully solvothermally synthesized a water stable microporous MOF material with a (5,8)-connected rod-packing network topology. Compound **1** exhibits satisfactory chemical stability, especially water stability, as well as certain adsorption performance for small gases and good selectivity for CO_2/CH_4. The excellent stability of compound **1** is essential for its practical industrial applications in the field of gas separation in the near future.

Conflicts of interest

There are no conflicts to declare.

Acknowledgements

This work was supported by the National Natural Science Foundation of China (No. 21771078 and 21621001).

Notes and references

1 (*a*) H. C. Zhou, J. R. Long and O. M. Yaghi, *Chem. Rev.*, 2012, **112**, 673; (*b*) H. C. Zhou and S. Kitagawa, *Chem. Soc. Rev.*, 2014, **43**, 5415; (*c*) B. Li, H. M. Wen, Y. Cui, W. Zhou, G. Qian and B. Chen, *Adv. Mater.*, 2016, **28**, 8819; (*d*) Y. Cui, B. Li, H. He, W. Zhou, B. Chen and G. Qian, *Acc. Chem. Res.*, 2016, **49**, 483; (*e*) Q. G. Zhai, X. Bu, C. Mao, X. Zhao, L. Daemen, Y. Cheng, A. J. Ramirez-Cuesta and P. Feng, *Nat. Commun.*, 2016, **7**, 13645; (*f*) B. Li, H. M. Wen, Y. Cui, W. Zhou, G. Qian Rogow, J. A. Mason, T. M. McDonald, E. D. Bloch, Z. R. Herm, T. H. Bae and J. R. Long, *Chem. Rev.*, 2012, **112**, 724–781; (*g*) X. Luo, Y. Cao, T. Wang, G. Li, Y. Yang, Z. Xu, J. Zhang, Q. Huo, Y. Liu and M. Eddaoudi, *J. Am. Chem. Soc.*, 2016, **138**, 786–789.

2 (*a*) K. Adil, Y. Belmabkhout, R. S. Pillai, A. Cadiau, P. M. Bhatt, A. H. Assen, G. Maurin and M. Eddaoudi, *Chem. Soc. Rev.*, 2017, **46**, 3402–3430; (*b*) R. Banerjee, A. Phan, B. Wang, C. Knobler, H. Furukawa, M. O'Keeffe and O. M. Yaghi, *Science*, 2008, **319**, 939–943; (*c*) J.-R. Li, J. Sculley and H.-C. Zhou, *Chem. Rev.*, 2012, **112**, 869–932; (*d*) Z. J. Zhang, Y. G. Zhao, Q. H. Gong, Z. Li and J. Li, *Chem. Commun.*, 2013, **49**, 653–661; (*e*) M. P. Suh, H. J. Park, T. K. Prasad and D.-W. Lim, *Chem. Rev.*, 2012, **112**, 782–835; (*f*) X.-F. Wang, Y.-B. Zhang, H. Huang, J.-P. Zhang and X.-M. Chen, *Cryst. Growth Des.*, 2008, **8**, 4559–4563; (*g*) X.-F. Wang, Y.-K. Sun and S.-H. Wang, *Microporous Mesoporous Mater.*, 2013, **181**, 262–269.

3 (*a*) J. Y. Lee, O. K. Farha, J. Roberts, K. A. Scheidt, S. B. T. Nguyen and J. T. Hupp, *Chem. Soc. Rev.*, 2009, **38**, 1450–1459; (*b*) L. Ma, C. Abney and W. Lin, *Chem. Soc. Rev.*, 2009, **38**, 1248–1256; (*c*) M. Yoon, R. Srirambalaji and K. Kim, *Chem. Rev.*, 2012, **112**, 1196–1231; (*d*) Z. Weng, Y. Wu, M. Wang, J. Jiang, K. Yang, S. Huo, X.-F. Wang, Q. Ma, G. W. Brudvig, V. S. Batista, Y. Liang, Z. Feng and H. Wang, *Nat. Commun.*, 2018, **9**, 415.

4 (*a*) N. Ahmad, H. A. Younus, A. H. Chughtai and F. Verpoort, *Chem. Soc. Rev.*, 2015, **44**, 9–25; (*b*) P. Horcajada, R. Gref, T. Baati, P. K. Allan, G. Maurin, P. Couvreur, G. Ferey, R. E. Morris and C. Serre, *Chem. Rev.*, 2012, **112**, 1232–1268; (*c*) J. Wang, D. Ma, W. Liao, S. Li, M. Huang, H. Liu, Y. Wang, R. Xie and J. Xu, *CrystEngComm*, 2017, **19**, 5244–5250.

5 (*a*) W. P. Lustig, S. Mukherjee, N. D. Rudd, A. V. Desai, J. Li and S. K. Ghosh, *Chem. Soc. Rev.*, 2017, **46**, 3242–3285; (*b*) L. Basabe-Desmonts, D. N. Reinhoudt and M. Crego-Calama, *Chem. Soc. Rev.*, 2007, **36**, 993–1017; (*c*) A. J. Lan, K. H. Li, H. H. Wu, D. H. Olson, T. J. Emge, W. Ki, M. C. Hong and J. Li, *Angew. Chem., Int. Ed.*, 2009, **48**, 2334–2338.

6 (*a*) E. Coronado and G. Minguez Espallargas, *Chem. Soc. Rev.*, 2013, **42**, 1525–1539; (*b*) J. Wang, X. Jing, Y. Cao, G. Li, Q. Huo and Y. Liu, *CrystEngComm*, 2015, **17**, 604; (*c*) X.-W. Wu, F. Pan, D. Zhang, G.-X. Jin and J.-P. Ma, *CrystEngComm*, 2017, **19**, 5864–5872.

7 (*a*) K. Sumida, D. L. Rogow, J. A. Mason, T. M. McDonald, E. D. Bloch, Z. R. Herm, T.-H. Bae and J. R. Long, *Chem. Rev.*, 2012, **112**, 724–781; (*b*) J.-R. Li, R. J. Kuppler and H.-C. Zhou, *Chem. Soc. Rev.*, 2009, **38**, 1477; (*c*) R. E. Morris and P. S. Wheatley, *Angew. Chem., Int. Ed.*, 2008, **47**, 4966; (*d*) J. Yu, L.-H. Xie, J.-R. Li, Y. Ma, J. M. Seminario and P. B. Balbuena, *Chem. Rev.*, 2017, **117**, 9674–9754.

8 (*a*) S. Yao, X. Sun, B. Liu, R. Krishna, G. Li, Q. Huo and Y. Liu, *J. Mater. Chem. A*, 2016, **4**, 15081–15087; (*b*) D. Wang, T. Zhao, G. Li, Q. Huo and Y. Liu, *Dalton Trans.*, 2014, **43**, 2365–2368.

9 H. Li, M. Eddaoudi, M. O'Keeffe and O. M. Yaghi, *Nature*, 1999, **402**, 276.

10 (*a*) L. Huang, H. Wang, J. Chen, Z. Wang, J. Sun, D. Zhao and Y. Yan, *Microporous Mesoporous Mater.*, 2003, **58**, 105; (*b*) P. M. Schoenecker, C. G. Carson, H. Jasuja, C. J. J. Flemming and K. S. Walton, *Ind. Eng. Chem. Res.*, 2012, **51**, 6513.

11 (*a*) C. Wang, X. Liu, N. K. Demir, J. P. Chen and K. Li, *Chem. Soc. Rev.*, 2016, **45**, 5107–5134; (*b*) J. Canivet, A. Fateeva, Y. Guo, B. Coasne and D. Farrusseng, *Chem. Soc. Rev.*, 2014, **43**, 5594; (*c*) A. J. Howarth, Y. Liu, P. Li, Z. Li, T. C. Wang, J. T. Hupp and O. K. Farha, *Nat. Rev. Mater.*, 2016, **1**, 15018.

12 N. C. Burtch, H. Jasuja and K. S. Walton, *Chem. Rev.*, 2014, **114**, 10575–10612.

13 M. Kandiah, M. H. Nilsen, S. Usseglio, S. Jakobsen, U. Olsbye, M. Tilset, C. Larabi, E. A. Quadrelli, F. Bonino and K. P. Lillerud, *Chem. Mater.*, 2010, **22**, 6632–6640.

14 J. E. Mondloch, W. Bury, D. Fairen-Jimenez, S. Kwon, E. J. Demarco, M. H. Weston, A. A. Sarjeant, S. T. Nguyen, P. C. Stuir, O. K. Farha and J. T. Hupp, *J. Am. Chem. Soc.*, 2013, **135**, 10294–10297.

15 V. Bon, V. Senkovska and S. Kaskel, *Chem. Commun.*, 2012, **48**, 8407–8409.

16 D. Cunha, M. B. Yahia, S. Hall, S. R. Miller, H. Chevreau, E. ElkaÏm, G. Maurin, P. Horcajada and C. Serre, *Chem. Mater.*, 2013, **25**, 2767–2776.

17 (*a*) K. S. Park, Z. Ni, A. P. Cote, J. Y. Choi, R. Huang, F. J. Uribe-Romo, H. K. Chae, M. O'Keeffe and O. M. Yaghi, *Proc. Natl. Acad. Sci. U. S. A.*, 2006, **103**, 10186–10191; (*b*) F. Wang, H.-R. Fu, Y. Kang and J. Zhang, *Chem. Commun.*, 2014, **50**, 12065–12068; (*c*) F. Wang, Z.-S. Liu, H. Yang, Y.-X. Tan and J. Zhang, *Angew. Chem., Int. Ed.*, 2011, **50**, 450–453.

18 G. Ferey, C. Mellot-Draznieks, C. Serre, F. Millange, J. Dutour, S. Surble and I. Margiolaki, *Science*, 2005, **309**, 5743.

19 (*a*) A. Schoedel, M. Li, D. Li, M. O'Keeffe and O. M. Yaghi, *Chem. Rev.*, 2016, **116**, 12466–12535; (*b*) J.-W. Zhang, M.-C. Hu, S.-N. Li, Y.-C. Jiang and Q.-G. Zhai, *Dalton Trans.*, 2017, **46**, 836.

20 G. M. Sheldrick, *SHELXTL-NT, version 5.1*, Bruker AXS Inc., Madison, WI, 1997.

21 V. A. Blatov, A. P. Shevchenko and D. M. Proserpio, *Cryst. Growth Des.*, 2014, **14**, 3576–3586.

22 S. S. Nagarkar, S. M. Unni, A. Sharma, S. Kurungot and S. K. Ghosh, *Angew. Chem., Int. Ed.*, 2014, **53**, 2638–2642.

23 J. L. C. Rowsell and O. M. Yaghi, *J. Am. Chem. Soc.*, 2006, **128**, 1304–1315.

24 B. Chen, M. Eddaoudi, S. T. Hyde, M. O'Keeffe and O. M. Yaghi, *Science*, 2001, **291**, 1021–1023.

25 D.-X. Xue, Y. Belmabkhout, O. Shekhah, H. Jiang, K. Adil, A. J. Cairns and M. Eddaoudi, *J. Am. Chem. Soc.*, 2015, **137**, 5034–5040.

26 (*a*) Y. He, Z. Zhang, S. Xiang, F. R. Fronczek, R. Krishna and B. Chen, *Chem. Commun.*, 2012, **48**, 6493–6495; (*b*) Y. He, W. Zhou, R. Krishna and B. Chen, *Chem. Commun.*, 2012, **48**, 11813–11831; (*c*) H. X. Zhang, H. R. Fu, H. Y. Li, J. Zhang and X. Bu, *Chem. – Eur. J.*, 2013, **19**, 11527–11530.

27 (*a*) N. U. Qadir, S. A. M. Said and H. M. Bahaidarah, *Microporous Mesoporous Mater.*, 2015, **201**, 61; (*b*) J. L. C. Rowsell and O. M. Yaghi, *J. Am. Chem. Soc.*, 2006, **128**, 1304–1315; (*c*) A. L. Myers and J. M. Prausnitz, *AIChE J.*, 1965, **11**, 121.

28 (*a*) W. Lu, D. Yuan, J. Sculley, D. Zhao, R. Krishna and H. C. Zhou, *J. Am. Chem. Soc.*, 2011, **133**, 18126–18129; (*b*) S. D.

Burd, S. Ma, J. A. Perman, B. J. Sikora, R. Q. Snurr, P. K. Thallapally, J. Tian, L. Wojtas and M. J. Zaworotko, *J. Am. Chem. Soc.*, 2012, **134**, 3663–3666; (*c*) H. Zhao, Z. Jin, H. Su, J. Zhang, X. Yao, H. Zhao and G. Zhu, *Chem. Commun.*, 2013, **49**, 2780–2782.

29 J. Li, X. Luo, N. Zhao, L. Zhang, Q. Huo and Y. Liu, *Inorg. Chem.*, 2017, **56**, 4141–4147.

30 X. Duan, Q. Zhang, J. Cai, Y. Yang, Y. Cui, Y. He, C. Wu, R. Krishna, B. Chen and G. Qian, *J. Mater. Chem. A*, 2014, **2**, 2628–2633.

